File ID	87685
Filename	Chapter 4: CHARGE MODIFICATION OF THE ENDOTHELIAL SURFACE LAYER MODULATES THE PERMEABLILITY BARRIER OF SMALL MESENTERIC ARTERIES

SOURCE (OR PART OF THE FOLLOWING SOURCE):

Type	Dissertation
Title	Wall permeability of isolated small arteries. Role of the endothelial surface layer
Author	P.M.A. van Haaren
Faculty	Faculty of Medicine
Year	2003

FULL BIBLIOGRAPHIC DETAILS:
http://dare.uva.nl/record/143889

chapter 4

4

CHARGE MODIFICATION OF THE ENDOTHELIAL SURFACE LAYER MODULATES THE PERMEABLILITY BARRIER OF SMALL MESENTERIC ARTERIES

4.1 ABSTRACT

We hypothesized that modulation of the effective charge density of the endothelial surface layer (ESL) results in altered arterial barrier properties to transport of anionic solutes. Rat mesenteric small arteries (d ~190 μm) were isolated, cannulated, perfused and superfused with MOPS-buffered physiological saline solutions. MOPS-solutions were of normal ionic strength (MOPS, IS = 162 mM), low ionic strength (LO-MOPS, IS = 81 mM), or high ionic strength (HI-MOPS, IS = 323 mM), to modulate ESL charge density (respectively normal, high or low ESL charge). Osmolarity of MOPS, LO-MOPS and HI-MOPS was kept constant at 297 mosmol, using additional glucose when necessary. Perfusate solutions were supplemented with 1% bovine serum albumin. Arteries were cannulated with a double-barreled θ-pipet on the inlet side and a regular pipet on the outlet side. After infusion of fluorescein-isothiocyanate (FITC)-labeled dextran of 50 kD (FITC-Δ50) and the endothelial membrane dye DiI, dynamics of arterial dye-filling were determined with confocal microscopy. ESL thickness, as determined from the initial exclusion zone for FITC-Δ50 on the luminal endothelial surface, was 6.3 ± 1.4 μm for LO-MOPS, 2.7 ± 1.0 μm for MOPS, and 1.1 ± 1.3 μm for HI-MOPS. At low ionic strength, FITC-Δ50 permeated into the ESL with a total ESL permeation time (τ_{ESL}) of 26 min, and at normal IS with a τ_{ESL} of 20 min. No apparent exclusion of FITC-Δ50 from the ESL could be observed at high IS. In conclusion, we demonstrate that modulation of solvent ionic strength influences the thickness and barrier properties of the ESL.

4.2 INTRODUCTION

The luminal surface of vascular endothelium is coated with highly negatively charged proteoglycans and glycosaminoglycans of the glycocalyx that contribute to the permselective barrier properties of the vascular wall. Several investigators have studied transvascular or glomerular transport of charged molecules (2;3;6-8;12;13;15-17;20;21). Well-known factors determining solute transport are size, conformation and charge of solute molecules. Most studies show diminished transport of anionic molecules in comparison to neutral molecules of similar size and conformation, whereas transport of cationic molecules is generally enhanced, although some contradictory results have also been reported (12;13;16).

Recently, Vink and Duling (26) showed that transport of solutes within the endothelial surface

layer (ESL, also known as the glycocalyx) of capillaries is dependent on size and charge of the solutes. In a previous study, we developed a model to study ESL transport of anionic solutes in small cannulated arteries (chapter 2). We found that a 2-3 μm thick endothelial surface layer (ESL) confines large anionic molecules (FITC-Δ148; 148 kD) to a core volume inside these arteries, while FITC-Δ50 (50 kD) is able to slowly permeate into this layer, and FITC-Δ4 (4 kD) relatively easily crosses the ESL and accumulates into the arterial wall.

Recently, Stace and Damiano (5;22) developed an electrochemical model to predict ESL transport of charged molecules. This model predicts partial exclusion of anionic tracers from the ESL and attenuated transport of these tracers into the ESL over time. Both the exclusion factor and the accumulation rate are predicted to depend on the volume density of fixed charges within the ESL and on the valence of solute tracers. According to the model, cations present in blood (partially) counterbalance fixed negative charges in the ESL and it was hypothesized that modulation of the ESL charge density by varying solvent ionic composition, provides an approach to determine the influence of ESL charge density on transvascular transport of anionic molecules.

In the present study we aimed to determine the influence of solvent ionic strength on ESL transport properties of anionic molecules in cannulated small arteries. We hypothesized that modulation of ionic strength influences the effective charge density of the ESL and can thus result in altered barrier properties of the ESL to transport of anionic molecules. Transport kinetics were measured with confocal laser scanning microscopy (CLSM). We used MOPS-buffered physiological saline solutions with either normal ionic strength, low ionic strength (LO-MOPS), or with high ionic strength (HI-MOPS) to modulate ESL charge density.

4.3 MATERIALS AND METHODS

4.3.1 Artery preparation

All experiments were performed according to the institutional guidelines. Male Wistar rats (N=21, 200-250 g) were decapitated, the mesentery was excised and immediately put into cold (4 °C) MOPS-PSS (see *solutions*). A small artery was dissected from the mesentery and transported to the pressure myograph. Average internal diameter at 60 mmHg and full dilation was 189 ± 6 μm; no significant differences in diameter existed between the various groups of arteries in this study. Each rat provided one vessel. Other vessels or organs from the same rat were used in other experiments.

4.3.2 Myograph

The isolated artery was cannulated at one end with a double-barreled θ-cannula (World Precision Instruments Inc.), and at the other end with a regular glass cannula. The artery was pressurized and perfused with either MOPS-BSA, LO-MOPS-BSA or HI-MOPS-BSA (see *solutions*) at input and output pressures of respectively 65 and 55 mmHg by means of two Fairchild pressure regulators. This pressure difference resulted in a flow through the arteries of 3.4 ± 0.5 $\mu l \cdot min^{-1}$, as measured by a μFlow liquid mass flowmeter (Bronkhorst Hi-Tec Holland BV), resulting in an estimated wall shear stress of 1.0 ± 0.2 $dyne \cdot cm^{-2}$. The artery could be perfused with a solution containing fluorescent tracers via the second barrel of the θ-cannula. Fluorescent perfusate was also pressurized to 65 mmHg. The superfusate, 37 °C MOPS-PSS, LO-MOPS-PSS or HI-MOPS-PSS (see *solutions*) of which PO_2 was maintained at ambient values, was continuously recirculated with a rollerpump. The PCO_2 was not controlled since pH was buffered by MOPS. Under these conditions these arteries were without tone and maintained a constant diameter during the protocol.

4.3.3 Solutions

The MOPS-buffered physiological saline solution (MOPS-PSS) contained: NaCl (145 mM), KCl (4.7 mM), $MgSO_4$ (1.17 mM), NaH_2PO_4 (1.2 mM), $CaCl_2$ (2 mM), MOPS (3-[N-Morpholino] propanesulfonic acid) (3 mM), glucose (5 mM) and pyruvate (2 mM).

The low-ionic-strength solution LO-MOPS-PSS contained: NaCl (64.2 mM), KCl (4.7 mM), $MgSO_4$ (1.17 mM), NaH_2PO_4 (1.2 mM), $CaCl_2$ (2 mM), MOPS (3 mM), glucose (153.8 mM) and pyruvate (2 mM).

The high-ionic-strength solution HI-MOPS-PSS contained: NaCl (38.2 mM), Na_2SO_4 (89.5 mM), KCl (4.7 mM), $MgSO_4$ (1.17 mM), NaH_2PO_4 (1.2 mM), $CaCl_2$ (2 mM), MOPS (3 mM), glucose (5 mM) and pyruvate (2 mM).

Ionic strength (IS) of MOPS-PSS was 162 mM, of LO-MOPS-PSS 81 mM, and of HI-MOPS-PSS 323 mM (according to $IS \equiv \frac{1}{2}\Sigma c_i \cdot z_i^2$, where c_i is the concentration of ion i, and z_i is its valence). Osmolarity for all three solutions was 297 mosmol (according to osmolarity = $\Sigma \phi_i \cdot j_i \cdot c_i$, where ϕ_i is the osmotic coefficient of solute i, j_i is its number of particles formed upon dissociation, and c_i is its concentration). Perfusate MOPS-PSS, LO-MOPS-PSS and HI-MOPS-PSS were supplemented with 10 mg/ml bovine serum albumin (BSA). All chemicals were purchased from SIGMA. All solutions were adjusted to pH 7.35.

4.3.4 Confocal microscopy

Images were recorded with a Leica DM IRBE microscope equipped with a Leica TCS SP2 confocal unit. Arteries were visualized from below through a cover glass that formed the bottom of the cannulation chamber. Excitation was obtained by an Ar-ion laser using the 488 line. A 20× / 0.70 objective in combination with a zoom factor of 2 resulted in a pixelsize of 366 nm × 366 nm in the plane of focus. Green and red fluorescence were detected using a prism and adjustable slits in front of two photomultipliers (PMTs). Wavelength of the detected light ranged respectively from 500 to 530 nm (green) and from 625 to 750 nm (red). Crosstalk between both fluorescence channels was negligible. The detection pinhole was 20 μm wide. Optical section thickness was about 13 μm. In this protocol, most CLSM settings, including laser power, wavelength settings, and pinhole size, were identical for all experiments. However, high voltage settings for the PMTs were not identical for all experiments. Consequently, fluorescence intensity was not directly comparable for all the recorded images. Therefore, we normalized FITC-Δ50 fluorescence intensity to mid-luminal fluorescence before comparison between different experiments. Images were recorded at mid-plane of the arteries every 3 sec during the first 1.5 minutes of dye perfusion. During the remainder of the dye perfusion period (2-30 min) images were recorded every minute. Arteries were not illuminated between measurements in order to prevent phototoxic damage (25).

4.3.5 Optical light-spread functions

In order to quantify the effect of the optical transfer function of the microscope system on the measured dye distributions we developed a correction procedure as previously described and verified (chapter 2). Briefly, we characterized the optical transfer function by an optical light-spread function (LSF) that characterizes the blurring in the plane of focus perpendicular to the arterial wall. To determine the LSF we employed two methods: 1) from the fluorescence profile of FITC-Δ50 in a glass dummy, consisting of a microtube with an inner diameter of 167 μm and a wall thickness of 65 μm of which one end was glued to a θ-cannula using silicon glue. This dummy was used as a model for an artery with uniform luminal filling and no wall fluorescence; 2) from the fluorescence profile of the DiI labeling in the endothelial membranes (see *fluorescent probes*).

We estimated square-shaped FITC-Δ50 concentration profiles in the arteries whose convolution with the LSF match the measured arterial fluorescence profiles after 2-30 min of FITC-Δ50 perfusion. These concentration profiles were characterized by a shift X_s from the endothelial

position. Differences between results obtained with the LSF derived from the dummy or with the LSF derived from the DiI fluorescence peaks at the endothelium were small and never significant. This procedure allowed us to localize the FITC-Δ50 concentration distribution with respect to the endothelial position and to quantify FITC-Δ50 transport kinetics (chapter 2).

4.3.6 Image analysis

Profiles in radial direction were made of all fluorescence images, recorded at mid-plane, with the image analysis software ImageJ (NIH, USA). Measurement of the diameter of the arteries was based on the position of the endothelium, which was determined from the peak in the DiI fluorescence profiles, after subtraction of luminal DiI fluorescence (i.e. the profile after 1.5 min). FITC-Δ50 fluorescence profiles, normalized to mid-luminal fluorescence intensity, were quantified in a region spanning from 10 μm abluminally to 15 μm luminally of the endothelium.

4.3.7 Fluorescent probes

Fluorescein-isothiocyanate-labeled dextran of 50.7 kD (FITC-Δ50) was purchased from SIGMA and the lipophilic membrane tracer DiI (1,1'-dioctadecyl-3,3,3',3'-tetramethylindocarbocyanine perchlorate) from Molecular Probes. FITC-Δ50 was applied in a concentration of 45.0 mg FITC-Δ50 / liter, resulting in a concentration of $1.0 \cdot 10^{-6}$ M FITC. Labeling ratio for FITC-Δ50 was 0.004 FITC per glucose molecule, according to the distributor. Therefore, the net anionic charge on FITC-Δ50 is ~1.1/dextran. DiI was applied in a concentration of $1.0 \cdot 10^{-5}$ M. Once incorporated in the endothelial membrane, DiI will stay there for the remainder of the experiment. DiI is able to spread along the membrane of an endothelial cell, but it cannot migrate from one cell to another (9-11).

4.3.8 Statistics

Data are presented as means ± SEM. Parameters describing fluorescence profiles for the different solutions were compared using ANOVA and bonferroni post-hoc tests. Paired t-tests were used for the comparison of parameters at 2 min versus 30 min.

4.4 RESULTS

After cannulation, arteries were equilibrated at 37 °C for at least 30 minutes. Endothelial viability was tested by administration of 10^{-6} M acetylcholine (ACH) to the superfusate of

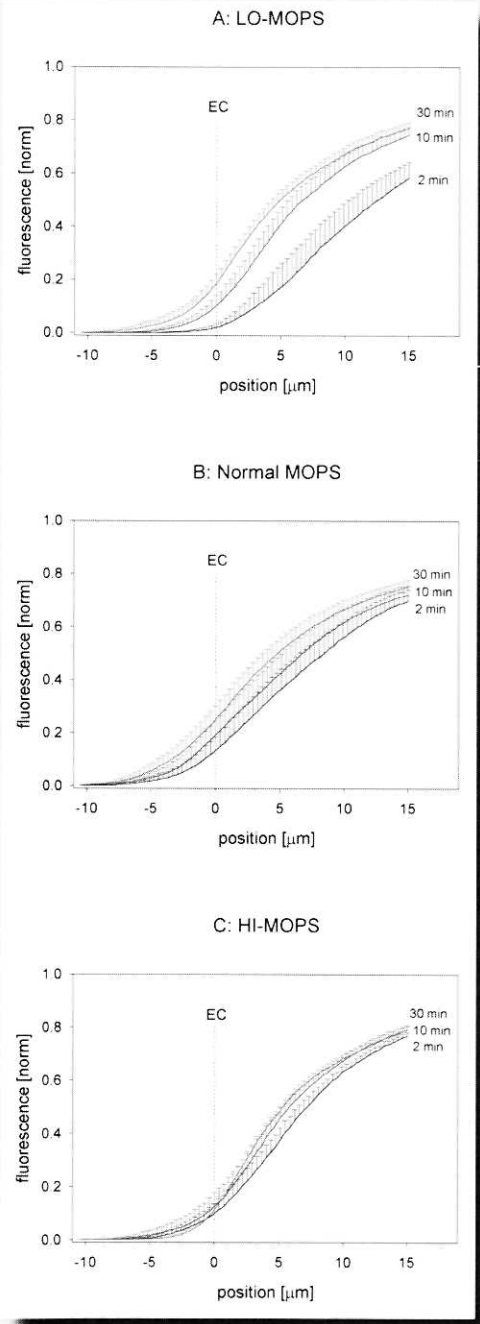

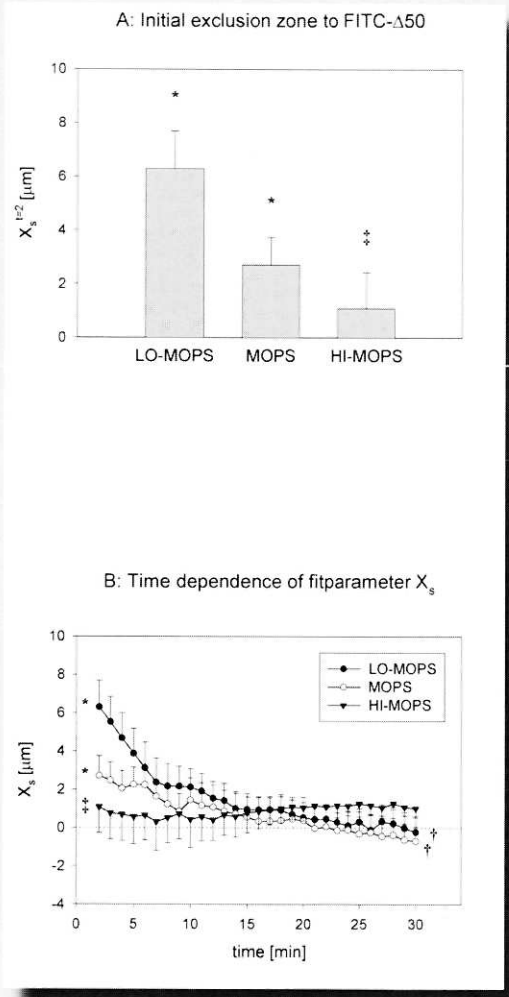

*Figure 4.2: A: Average value of fit parameter X_s after 2 min of FITC-Δ50 perfusion in the LO-MOPS, MOPS, and HI-MOPS experiments. B: Time dependence of parameter X_s from the fits of the fluorescence profiles of the LO-MOPS, MOPS and HI-MOPS experiments. Values are means ± SEM (n=7 experiments for each group; * significantly different from 0 μm; † $p<0.05$, 30 min vs. 2 min; ‡ $p<0.05$ vs. LO-MOPS).*

Figure 4.1: Kinetics of average normalized FITC-Δ50 fluorescence in a region from 10 μm abluminally to 15 μm luminally of the endothelium for arteries perfused and superfused with LO-MOPS (A), normal MOPS (B), or HI-MOPS (C). Fluorescence was normalized to mid-luminal fluorescence. Position of the endothelium was determined from peak DiI fluorescence and is depicted with the dotted lines. Negative x-values indicate abluminal from the endothelium (arterial wall), positive values indicate luminal from the endothelium. Profiles are mean values ± SEM (n=7 experiments for each group).

arteries,preconstricted with 10^{-6} M noradrenaline. Ionic strength did not affect dilation in response to ACH (LO-MOPS: 58.9 ± 9.1 %, MOPS: 68.5 ± 8.9 %, HI-MOPS: 53.8 ± 11.2 %, P=NS). Further measurements were obtained without preconstriction at full dilation.

To determine the spatial distribution of FITC-Δ50 over time, we measured fluorescence profiles from the recorded images during 30 min of dye perfusion for 7 arteries in each group (LO-MOPS, MOPS, and HI-MOPS). Figure 4.1 provides the average fluorescence profiles in a region extending between 15 μm at the luminal side and 10 μm at the abluminal side of the endothelium, of cannulated arteries perfused and superfused with LO-MOPS (fig. 4.1A), normal MOPS (fig. 4.1B), or HI-MOPS (fig. 4.1C). The position of the endothelium (EC) as determined from peak DiI fluorescence, is taken as position 0 μm, and is depicted with the vertical dotted lines. Figure 4.1 demonstrates that the development of the fluorescence profiles is slowest for LO-MOPS, faster for MOPS, and very fast for HI-MOPS, while after 30 min of dye perfusion approximately identical fluorescence distributions are accomplished for the different groups of arteries.

Figure 4.2A shows the average initial distance of FITC-Δ50 from the endothelial position, representing the dimension of the ESL for the different ionic strength conditions. Initial X_s for LO-MOPS, 6.3 ± 1.4 μm ($P<0.05$ vs. 0 μm), was significantly higher than for HI-MOPS, 1.1 ± 1.3 μm (P=NS vs. 0 μm).

Figure 4.2B shows the time dependence of X_s for LO-MOPS, MOPS and HI-MOPS, representing the time-dependent permeation of FITC-Δ50 into the ESL for the different ionic strength conditions. For LO-MOPS, X_s decreased significantly during 30 min of dye perfusion from 6.3 ± 1.4 μm after 2 min to -0.2 ± 0.8 μm (P=NS vs. 0 μm) after 30 min, with a total ESL permeation time (τ_{ESL}) of ~26 min. For MOPS, X_s decreased significantly from 2.7 ± 1.0 μm ($P<0.05$ vs. 0 μm) after 2 min to -0.7 ± 0.7 μm (P=NS vs. 0 μm) after 30 min, with a τ_{ESL} of ~20 min. For HI-MOPS, no significant change in X_s occurred (from 1.1 ± 1.3 μm after 2 min to 1.0 ± 0.5 μm after 30 min), indicating no detectable exclusion of FITC-Δ50 from the ESL.

4.5 DISCUSSION

We demonstrate that modulation of solvent ionic strength affects the dimension of the endothelial surface layer (ESL) and the kinetics of FITC-Δ50 transport into the ESL of isolated, cannulated rat mesenteric small arteries.

4.5.1 Comparison to literature

4.5.1.1 Transvascular transport of charged molecules.

Many authors have investigated transvascular or glomerular transport properties of charged molecules (2;3;6-8;12;13;15-17;20;21). Most studies involving charge show diminished transport of anionic molecules in comparison to neutral molecules of similar size and conformation, whereas transport of cationic molecules is generally enhanced, but some contradictory results have also been reported (12;13;16). Although a diminished transport of anionic solutes is in agreement with the presence of fixed negative charges on the luminal endothelial surface, the exact dimension of the endothelial structures carrying these negative charges has not yet been determined satisfactorily. Imaging of the fixed negative charges after staining with cationic probes (1;14;18;19;23), shows that the charges are mainly located in membrane bound structures (glycocalyx) of the ESL such as glycoproteins and proteoglycans, but these techniques usually fail to obtain insight in the true *in vivo* dimensions of the charge carrying structures.

4.5.1.2 The endothelial surface layer and transport of anionic molecules.

Evidence for the existence of a relatively thick (~0.5 μm) endothelial surface layer (ESL) in capillaries was provided by Vink and Duling (25;26). These authors showed that transport of solutes within the ESL of capillaries is strongly dependent on size and charge of the solutes. Recently, we determined transport properties of fluorescein-isothiocyanate (FITC)-labeled dextrans (FITC-Δs) in cannulated small arteries of ~150 μm in diameter (chapter 2). We found that a 2-3 μm thick ESL confines large anionic molecules (FITC-Δ148; 148 kD) to a core volume inside the arteries, while FITC-Δ50 (50 kD) was able to slowly penetrate this layer, and FITC-Δ4 (4 kD) was able to pass the ESL and accumulate in the arterial wall within 30 minutes.

To study transport properties of anionic molecules through the capillary ESL, Stace and Damiano (5;22) developed an electrochemical model. This model predicts the initial exclusion of anionic tracers from the ESL and the transport of these tracers into the ESL over time. Both issues are dependent on the charge density of the ESL and on the valence of the tracers. According to this model cations present in blood partially counterbalance fixed negative charges in the ESL. These authors proposed to use variations in perfusate ionic composition to modulate ESL charge density and thereby influence ESL transport of anionic tracers. It was predicted that a 2-fold decrease in ionic strength would result in a 2-fold increase in ESL charge density and a 2-fold increase in the voltage differential over the luminal blood-ESL interface that forms the actual physical barrier to

transport of anionic molecules. This voltage differential was predicted to be in the order of 0.1-1 mV in plasma or normal saline, but the practical limitations of direct measurement of these voltage gradients over the ESL are prohibitive (5;22). Furthermore, an increase in ionic strength was predicted to decrease ESL charge density and to attenuate exclusion of anionic molecules from the ESL.

Our data demonstrate an ionic-strength-dependent ESL thickness (figure 4.2A). Assuming that the total amount of charge carrying proteoglycan fiber-structures in the ESL is constant, this implies condensation of these fibers inside the ESL at high ionic strength and extension of the fibers at low ionic strength. This concept would be consistent with the differences in ESL thickness and in kinetics of FITC-Δ50 permeation into the ESL observed in the present study for the different ionic strength conditions.

Direct conformational changes in red blood cell (RBC) glycocalyx due to variations in ionic strength have been reported by Wolf and Gingell (27). These authors demonstrated that the RBC glycocalyx is swelling roughly by a factor ~2.2 as ionic strength falls by a factor 4. The swelling effects at low ionic strength might explain the large exclusion zone to FITC-Δ50 when using LO-MOPS observed in the present study. Here, the dimension of the exclusion zone increased by a factor ~2.3 as ionic strength was decreased 2-fold (LO-MOPS compared with normal MOPS), while ESL thickness decreased by a factor ~2.5 as ionic strength was doubled (HI-MOPS compared with normal MOPS).

ESL volume is determined by a dynamic equilibrium of water movement into the ESL due to interactions between the charge carrying structures of the glycocalyx, free plasma ions and other charged molecules present in the perfusate and the hydrostatic pressure of the perfusate (5). Upon modification of one of these factors, the ESL will adapt its structural organization to a new dynamic equilibrium. Therefore, modulation of perfusate and superfusate ionic strength is likely to result in dimensional changes of the ESL as well as changes in ESL charge distribution, both affecting ESL permeability properties.

4.5.1.3 Ionic strength modulation of vascular permeability.

Sörensson and coworkers (20;21) have studied the influence of perfusate ionic strength on the charge selectivity of the glomerular capillary wall. These authors demonstrated that lowering ionic strength by 4.5-fold reduced the fractional clearance of several anionic tracers by ~1.5-fold, which was attributed to a reduction in radius of the small pores responsible for the exchange and to a reduction in the charge density of the glomerular barrier. The latter seems to be due to volume

alterations of the 'charged gel' that covers endothelial cells. A 1.9-fold increase in ionic strength resulted in a slightly increased fractional clearance of anionic tracers. Furthermore, Granger and coworkers (8) demonstrated that neutralization of the negative fixed charges on the intestinal capillary wall by infusion of polycations induces a ~6-fold increase in permeability to fluid and a ~4-fold increase in protein clearance.

Based on these findings, we hypothesized that solvent ionic strength influences the barrier properties of the arterial ESL. At normal physiological ionic strength, cations partially neutralize fixed negative charges within the ESL, but a net negative ESL charge remains present that impairs transport of anionic molecules. At higher ionic strength the fixed charges are more neutralized, which results in reduced ability of the ESL to extend into the vascular lumen and reduced impairment of transport of anionic molecules. At low ionic strength the neutralization of the fixed charges is weaker, thus the ESL might extend further into the lumen and might more severely impair transport of anionic molecules. We found a longer ESL permeation time for LO-MOPS in comparison to MOPS, indicating that a reduction in IS resulted in a greater impairment of FITC-Δ50 transport across the ESL. We assumed that the situation with normal MOPS was more or less representative for the normal physiological charge distribution conditions, since the concentration of all present ions and thus the ionic strength are almost equal for MOPS and normal plasma.

4.5.2 Criticism of the method

Due to the size of the arteries used, a long working distance objective with relatively low numerical aperture was needed. Even in confocal microscopy, this results in blurring of the images and complicates the localization of the fluorescent tracers. In order to circumvent this complication, we previously developed and verified a correction procedure to estimate the concentration distribution of the tracers inside the cannulated arteries (chapter 2). Briefly, we characterized the blurring of the images in the plane of focus perpendicular to the arterial wall by an optical light-spread function (LSF), which was derived from the fluorescence profiles of the tracer inside a glass dummy or from the fluorescence profile of the DiI labeling in the endothelium. Concentration profiles were then estimated by comparing their convolution with the LSF to the observed arterial fluorescence profiles. We assumed square-shaped concentration profiles, characterized by a shift (X_s) from the endothelial position. Differences between results obtained with the LSF derived from the dummy or with the LSF derived from the DiI fluorescence peaks at the endothelium were small and never significant.

We extended the correction procedure by fitting all fluorescence profiles measured from 2-30 min of dye perfusion, whereas we only fitted the profiles after 30 minutes in the previous study (chapter 2). By obtaining X_s from 2-30 min of dye perfusion we were able to study the kinetics of FITC-Δ50 transport through the ESL and the dependence of these kinetics on solvent ionic strength. This led us to substantiate that ESL dimension, as determined from the luminal exclusion zone to FITC-Δ50 after 2 min of dye perfusion, as well as transport kinetics of FITC-Δ50 into the ESL are dependent on ionic strength. We did not obtain X_s for dye perfusion times shorter than 2 min, since this would be complicated due to inflow effects of FITC-Δ50 into the artery. Consequently, it is difficult to quantify the development of the fluorescence profiles and FITC-Δ50 transport through the ESL before 2 min. Therefore, it is difficult to determine whether ESL dimension or ESL transport properties or both have been influenced by solvent ionic strength during the first 2 min of dye perfusion. Nevertheless, from extrapolation of X_s to 0 min, we feel that our conclusions about the influence of ionic strength on dimension as well as transport properties of the ESL are valid, whose conclusions are in agreement with the hypotheses and knowledge from literature about the influence of ionic strength on ESL dimension and transport properties, as discussed above.

4.5.3 Implications of the study

An endothelial surface layer of several micrometers in thickness carrying fixed negative charges, will impair the movement of anionic solutes passing through or interacting with the vessel wall. Damage to the ESL by for example oxidative stress (4;24-26) or modification of its properties by changes in the ionic composition of the environment might alter vascular permeability properties to negatively charged proteins such as albumin.

4.6 REFERENCES

1. **Baldwin,A.L., N.Z.Wu, and D.L.Stein.** Endothelial surface charge of intestinal mucosal capillaries and its modulation by dextran. *Microvasc Res* 42: 160-178, 1991.
2. **BÅrenner,B.M., T.H.Hostetter, and H.D.Humes.** Glomerular permselectivity: barrier function based on discrimination of molecular size and charge. *Am J Physiol-Renal* 234: F455-F4601978.
3. **Chang,R.L., W.M.Deen, C.R.Robertson, and B.M.Brenner.** Permselectivity of the glomerular capillary wall: III. Restricted transport of polyanions. *Kidney Int* 8: 212-218, 1975.
4. **Constantinescu,A.A., H.Vink, and J.A.E.Spaan.** Elevated capillary tube hematocrit reflects degradation of the glycocalyx by oxidized low density lipoproteins. *Am J Physiol-Heart C* 280: H1051-H10572001.
5. **Damiano,E.R. and T.M.Stace.** A mechano-electrochemical model of radial deformation of the capillary glycocalyx. *Biophys J* 82: 1153-1175, 2002.
6. **Deen,W.M., M.J.Lazzara, and B.D.Myers.** Structural determinants of glomerular permeability. *Am J Physiol-Renal* 281: F579-F5962001.
7. **Deen,W.M., B.Satvat, and J.M.Jamieson.** Theoretical model for glomerular filtration of charged solutes. *Am J Physiol-Renal* 238: F126-F1391980.
8. **Granger,D.N., P.R.Kvietys, M.A.Perry, and A.E.Taylor.** Charge selectivity of rat intestinal capillaries. Influence of polycations. *Gastroenterology* 91: 1443-1446, 1986.
9. **Haugland,R.P.** Handbook of Fluorescent Probes and Research Chemicals. Eugene, *OR: Molecular Probes, Inc.*, 1996,
10. **Hiscox,S. and W.G.Jiang.** Quantification of tumour cell-endothelial cell attachment by 1,1'-dioctadecyl-3,3,3',3'-tetramethylindocarbocyanine (DiI). *Cancer Lett.* 112: 209-217, 1997.
11. **Honig,M.G. and R.I.Hume.** Fluorescent carbocyanine dyes allow living neurons of identified origin to be studied in long-term cultures. *J Cell Biol* 103: 171-187, 1986.
12. **Osicka,T.M. and W.D.Comper.** Glomerular charge selectivity for anionic and neutral horseradish peroxidase. *Kidney Int* 47: 1630-1637, 1995.
13. **Osicka,T.M. and W.D.Comper.** Tubular inhibition destroys charge selectivity for anionic and neutral horseradish peroxidase. *Biochim Biophys Acta* 1381: 170-178, 1998.
14. **Palade,G.E., M.Simionescu, and N.Simionescu.** Differentiated microdomains on the luminal surface of the capillary endothelium. *Biorheology* 18: 563-568, 1981.
15. **Parker,J.C., M.Miniati, R.Pitt, and A.E.Taylor.** Interstitial distribution of charged macromolecules in the dog lung: a kinetic model. *Ann Biomed Eng* 15: 157-172, 1987.
16. **Perry,M.A., J.N.Benoit, P.R.Kvietys, and D.N.Granger.** Restricted transport of cationic macromolecules across intestinal capillaries. *Am J Physiol-Gastr* L 245: G568-G5721983.
17. **Rennke,H.G., Y.Patel, and M.A.Venkatachalam.** Glomerular filtration of proteins: clearance of anionic, neutral, and cationic horseradish peroxidase in the rat. *Kidney Int* 13: 278-288, 1978.
18. Simionescu,M., N.Simionescu, J.E.Silbert, and G.E.Palade. Differentiated microdomains on the luminal surface of the capillary endothelium. II. Partial characterization of their anionic sites. *J Cell Biol* 90: 614-621, 1981.
19. **Simionescu,N., M.Simionescu, and G.E.Palade.** Differentiated microdomains on the luminal surface of the capillary endothelium. I. Preferential distribution of anionic sites. *J Cell Biol* 90: 605-613, 1981.
20. **Sorensson,J., M.Ohlson, and B.Haraldsson.** A quantitative analysis of the glomerular charge barrier in the rat. *Am J Physiol-Renal* 280: F646-F6562001.
21. **Sorensson,J., M.Ohlson, K.Lindstrom, and B.Haraldsson.** Glomerular charge selectivity for horseradish peroxidase and albumin at low and normal ionic strengths. *Acta Physiol Scand* 163: 83-91, 1998.
22. **Stace,T.M. and E.R.Damiano.** An electrochemical model of the transport of charged molecules through the capillary glycocalyx. *Biophys J* 80: 1670-1690, 2001.
23. **Ueda,H., K.Takehana, Eerdunchaolu, K.Iwasa, O.Fujimori, and S.Shimada.** Electron microscopic cytochemical studies of anionic sites in the rat spleen. *J Vet Med Sci* 63: 287-291, 2001.
24. Vink,H., A.A.Constantinescu, and J.A.E.Spaan. Oxidized lipoproteins degrade the endothelial surface layer - Implications for platelet-endothelial cell adhesion. *Circulation* 101: 1500-1502, 2000.
25. **Vink,H. and B.R.Duling.** Identification of distinct luminal domains for macromolecules, erythrocytes, and leukocytes within mammalian capillaries. *Circ Res* 79: 581-589, 1996.
26. **Vink,H. and B.R.Duling.** Capillary endothelial surface layer selectively reduces plasma solute distribution volume. *Am J Physiol-Heart C* 278: H285-H2892000.
27. **Wolf,H. and D.Gingell.** Conformational response of the glycocalyx to ionic strength and interaction with modified glass surfaces: study of live red cells by interferometry. *Journal of Cell Science* 63: 101-112, 1983